Journal of Optoelectronics and Advanced Materials Vol. 6, No. 3, September 2004, p. 1001 - 1004

PREISACH-NÉEL TYPE MODEL FOR NANOSTRUCTURED MAGNETIC MATERIALS

A. Sava*, A. Stancu

"Alexandru Ioan Cuza" University, Faculty of Physics, Department of Electricity and Physical Electronics, 11, Carol I Blvd., Iasi, 700506, Romania

In this paper we present a new Preisach-Néel type model that can be successfully applied to simulate magnetisation processes of nanostructured magnetic materials. Taking into account the results of micromagnetic simulations, this model uses a Preisach distribution of interaction fields obtained by superposition of two Gaussian distributions. The amplitudes of the two distributions are dependent on the total magnetic moment of the sample. Therefore, we can take into account, in a very simple manner, state dependent interaction field distributions. The model was used to simulate temperature dependent magnetisation processes like the Zero Field Cooled (ZFC). The results show the ZFC dependence on the statistical and mean field interactions.

(Received April 21, 2004; accepted June 22, 2004)

Keywords: Preisach-Néel model, Thermal activation, Interparticle interactions

1. Introduction

The effect of magnetic interactions between particles on the properties of the nanostructured magnetic materials is a very disputed problem. In order to analyse the presence of interparticle interactions effects in such systems, many magnetisation processes were proposed. In systems where the remanent magnetic moment is usually considered time independent (relaxation effects are negligible), the magnetisation processes that are frequently used are the remanent curves: IRM (isothermal remanent magnetisation) and DCD (DC demagnetisation) processes [1,2]. With this data one calculates the well-known Henkel plot [3] and deltaM plot [4] to evaluate the interaction field distribution. When the size of particles becomes smaller, relaxation effects become important and other magnetisation processes, temperature and time dependent, reflect essentially the magnetic properties: the Zero Field Cooled (ZFC) magnetisation [5] and the Field Cooled (FC) magnetisation.

Various types of models were designed in order to explain complex magnetisation processes in systems of magnetic particles where the interactions between particles cannot be neglected [6,7]. Recent micromagnetic results have shown that the inter-particle interactions are statistically distributed and that both the average value and standard deviation of the interaction field distribution are state dependent [8]. We have shown that a two-peaks interaction fields distribution with the amplitude dependent on the magnetic moment of the sample can be used efficiently to account for this complex behaviour of the interactions. Using a Preisach-Néel model proposed by Roshko et al. [9,10], we consider this two-peaks interaction field distribution [11]. The new model is tested on ZFC processes in particulate ferromagnetic systems with different packing ratio.

2. Preisach-Néel type model

The scalar Preisach model [12] decomposes all magnetic systems into a collection of bistable subsystems. Each subsystem is characterized by a rectangular response function like that shown in Fig. 1(a), with two states $\Phi = \pm 1$, corresponding to the two discrete orientation of the

* Corresponding author: ancasaca@yahoo.com

subsystem moment, and two critical instability fields (H_α, H_β). The coercive field is: $h_c = (H_\alpha - H_\beta)/\sqrt{2}$ and the characteristic interaction field: $h_i = -(H_\alpha + H_\beta)/\sqrt{2}$. The shift field h_S measures the asymmetry caused by the interaction fields: $h_i = -h_s$. The equivalent zero field energy level diagram shown in Fig.1(b) is an asymmetric double well, with two energy barriers $W_+ = -H_\beta = h_c + h_i$ and $W_- = H_\alpha = h_c - h_i$, which inhibit transitions between the two local minima and block moment reorientation. The magnetic moment was normalized at the saturation magnetic moment of the sample.

In order to excite transitions between the two configurations, one must supply energy to the subsystem. In particular, the application of a positive external field h_a will modify the energy barriers and will stabilize the $\Phi = +1$ state and destabilize the $\Phi = -1$ state, as shown in Fig.1(c). Therefore, all the subsystems for which $0 < h_c - h_i < h_a$ $(0 \le H_\alpha \le h_a)$, will jump discontinuously from the state $\Phi = -1$ to the state $\Phi = +1$. Transitions may also be induced thermally if the subsystem is in contact with a heat bath at temperature T. For an experiment with a characteristic time constant t_{exp}, all energy barriers $W \le W^* = k_B T \ln(t_{exp}/\tau_0)$ will be thermally activated [13].

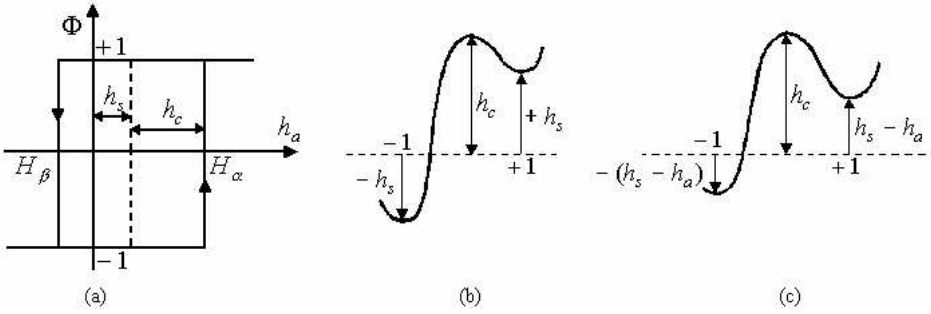

Fig. 1. (a) An elementary Preisach hysteresis loop. (b) The energy level diagram in zero applied field. (c) The energy level diagram in a positive applied field h_a>0.

Thermal transitions can be described by an equivalent thermal field $h_T^* = W^*$. The presence of thermal fluctuations means that transitions can occur in subsystems for which h_a is subcritical, so that all subsystems with $h_a < H_\alpha < h_a + h_T^*$ will be thermally activated into the state $\Phi = +1$ and all those with $h_a - h_T^* < H_\beta < h_a$ will be thermally activated into the state $\Phi = -1$. In this context, it is important to underline that only those subsystems for which both criteria are satisfied simultaneously will actually reach thermal equilibrium. Outside this region, thermal transitions are unidirectional and always drive the subsystem into the lowest energy state.

The subsystems are graphically represented in the Preisach plane, which uses the characteristic fields (H_α, H_β) and (h_c, h_i) to define rectangular coordinate axes. Each subsystem represents a point in this plane, and the distribution of subsystems is described by Preisach distribution $p(h_c, h_i)$. The instability conditions for the subsystems are lines in the Preisach plane, which separate the plane into thermally blocked (in $\Phi = +1$ or $\Phi = -1$ states) and thermally activated regions (Fig. 2).

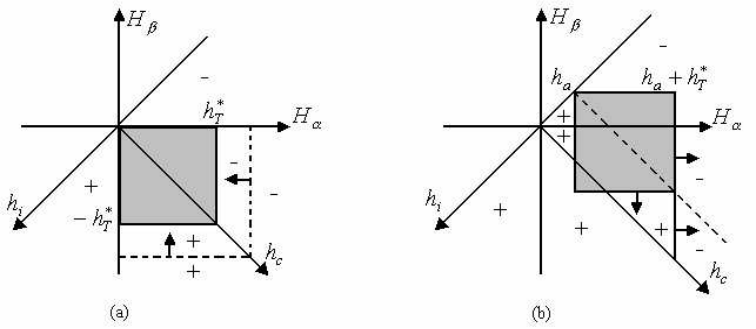

Fig. 2. The ZFC process in the Preisach plane. (a) The plus and minus signs indicate the blocked subsystems into one of the states $\Phi = \pm 1$. The shading region indicates the SP subsystems. (b) Warming in a positive field.

We have simulated with this model the ZFC process for a system of interacting ferromagnetic particles. The system is first heated in zero applied field to a temperature, which is high enough to ensure that all particles are in thermal equilibrium (superparamagnetic state, denoted SP). In terms of the model, this requires a thermal field h_T^*, which exceeds all the subsystem energy barriers. The system is then cooled in zero applied field and each subsystem will pass through a characteristic temperature T_B at which h_T^* is equal to the larger of its energy barriers. At this temperature, the larger energy barrier will become thermally inactive. However, the smaller barrier will continue to be thermally active and thermal fluctuations will empty the higher, metastabile energy level. For subsystems with $h_i < 0$, the blocking condition is $H_\alpha = h_T^*$. Fig. 2(a) shows a graphical representation of the ZFC process in the Preisach plane and Fig. 2(b) the warming in a positive field. The blocking boundaries are straight lines which separate those subsystems which are frozen into the $\Phi = +1$ or $\Phi = -1$ states, from those in the shaded region which are in thermal equilibrium and continue to exhibit the SP response $\Phi_{equ} = \tanh(h_i / k_B T) = \tanh(h_i \alpha / h_T^*)$, where $\alpha = \ln(t_{\exp} / \tau_0)$ is the time dependent factor of the thermal field h_T^*.

If the system is cooled in zero field to $T = 0$, where a positive field $h_a > 0$ is applied, and then warmed to a temperature T, all subsystems with $0 < H_\alpha < h_a + h_T^*$ will be activated to $\Phi = +1$ and those with $h_a - h_T^* < H_\beta < h_a$ will be activated to $\Phi = -1$ state.

The Preisach distribution is described by the product of two statistically independent distributions:

$$p(h_c, h_i) = p_c(h_c, h_{c0}) \cdot p_i(h_i, h_{i0}) \tag{1}$$

where $p_c(h_c, h_{c0})$ is the distribution of coercive fields and $p_i(h_i, h_{i0})$ is the distribution of interaction fields. The distributions are normalized at the saturation magnetic moment of the sample.

The coercive field distribution is given by:

$$p_c = \frac{1}{\sqrt{2\pi} h_{c\sigma}} \exp\left[-\frac{(h_c - h_{c0})^2}{2h_{c\sigma}^2} \right] \tag{2}$$

and the double Gaussian interaction field distribution is given by [10]:

$$p_i(h_i, h_{i0}) = \frac{1}{\sqrt{2\pi} h_{i\sigma}} \left\{ \frac{1+m}{2} \exp\left[-\frac{(h_i - h_{i0})^2}{2h_{i\sigma}^2} \right] + \frac{1-m}{2} \exp\left[-\frac{(h_i + h_{i0})^2}{2h_{i\sigma}^2} \right] \right\} \tag{3}$$

where m is the normalized magnetic moment and $h_{c\sigma}$, $h_{i\sigma}$ are the distributions dispersions.

The magnetic moment was calculated by superposing the responses $\Phi(h_c, h_i)$ of all subsystems, using the Preisach diagram from Fig.2:

$$m = \int_{-\infty}^{+\infty} \int_{0}^{+\infty} p(h_c, h_i) \Phi(h_c, h_i) dh_c dh_i \tag{4}$$

3. Numerical simulations

Fig. 3(a and b) shows the temperature dependence of ZFC moment in an applied field $h_a = 0.02$. The experimental time parameter $\alpha = \ln(t_{\exp} / \tau_0) = 25$ was chosen to correspond to typical dc measuring times $t_{\exp} \approx 10^2 - 10^3 s$, supposing $\tau_0 = 10^{-9} s$. First, Fig.3(a), was studied the influence of statistical interactions ($h_{i0} = const.$) and then, Fig.3(b), the influence of mean interaction field ($h_{i\sigma} = const.$) on ZFC curves. All field parameters were normalized to the mean coercive field h_{c0}.

The principal structural features of these curves are essentially identical to those observed experimentally [14]. In each case, $m_{ZFC}(T)$, exhibits a peak at a temperature $T_{\max}$. This peak is the result of competition between two opposing tendencies: as the temperature increases the thermal instability boundary $H_\alpha = h_a + h_T^*$ moves and favours thermal transitions from $\Phi = -1$ to $\Phi = +1$ state and the moment will increase, but in the same time the SP response will increase and will induce a decrease of the moment. The first mechanism dominates at low temperatures but it is exceeded at high temperatures by the increase of SP region and a peak ($T_{\max}, m_{\max}$) is obtained.

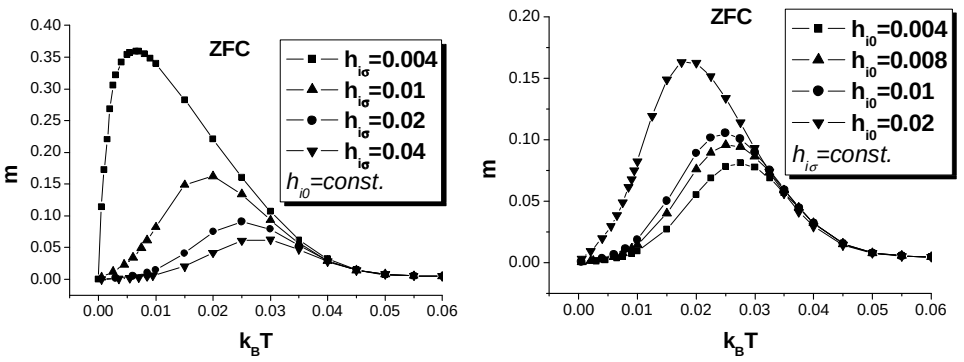

Fig. 3. The temperature dependence of ZFC moment in an applied field $h_a = 0.02$. (a) different dispersions of interaction fields: $h_{i\sigma} = 0.004, 0.01, 0.02, 0.04$, (b) different mean interaction fields: $h_{i0} = 0.004, 0.008, 0.01, 0.02$.

The increase of $T_{\max}$ is caused by the increase of energetic barriers with temperature. The behaviour of $m_{\max}$: decreases with $h_{i\sigma}$ and increases with h_{i0}, is the consequence of the sweeping through the Preisach distribution of the thermal instability boundary: high values of h_{i0} and small values of $h_{i\sigma}$ will favour $\Phi = +1$ state and will increase the magnetic moment.

4. Conclusions

In this paper we have developed a temperature dependent Preisach-Néel type model for nanostructured magnetic materials, using a double Gaussian interaction field distribution. The results show a strong dependence on the interaction intensity. It is important to observe that the position of the ZFC maximum, T_{max}, depends not only on the interaction dispersion but also on the mean field interactions if we take into account the correlation between the increase of the magnetic moment of the sample when the average value of the interaction field distribution is increasing and the standard deviation is decreasing. This effect has not been observed when the variation of the standard deviation was neglected. In a further paper we shall include in the model the nonlinear character of the energy barrier and the effect of the reversible magnetisation processes.

References

[1] A. Stancu, C. Papusoi, L. Spanu, J. Magn. Magn. Mater. **150**, 124 (1995).
[2] G. W. D. Spatt, P. R. Bissel, R. W. Chantrell, E. P. Wohlfarth, J. Magn. Magn. Mater. **75**, 309 (1988).
[3] O. Henkel, Phys. Stat. Sol. **7**, 919 (1964).
[4] P. E. Kelly, K. O'Grady, P. I. Mayo, R. W. Chantrell, IEEE Trans. Magn. **25**, 3881 (1989).
[5] R. W. Chantrell, M. El-Hilo, K. O'Grady, IEEE Trans. Magn. **27**, 3570 (1991).
[6] A. Stancu, L. Spinu , IEEE Trans. Magn. **34**(6), 3867 (1998).
[7] I. D. Borcia, L. Spinu, Al. Stancu, J. Optoelectron Adv. Mater. **5**(1), 355 (2003).
[8] D. Cimpoiesu, P. Postolache, A. Stancu, J. Appl. Phys. **93**(10), 6644 (2003).
[9] T. Song, M. Roshko, IEEE Trans. Magn. **36** (1), 223 (2000).
[10] P. D. Mitcher, E. Dan Dahlberg, E. E. Wesseling, R. M. Roshko, IEEE Trans. Magn. **32**(4), 3185 (1996).
[11] A. Stancu, L. Stoleriu, P. Postolache, M. Cerchez, **40**(4), 2113 (2004), IEEE Trans. Magn. (in press).
[12] F. Preisach, Z. Phys. **94**, 277 (1935).
[13] J. Souletie, J. Phys. **44**, 1095 (1983).
[14] J. L. Dormann, D. Fiorani, E. Tronc, Adv. Chem. Phys., **XCVIII**, (1997).